Title: CHK1 inhibition sensitises radioresistant head and neck cancers to paclitaxel-based chemoradiotherapy

Authors and affiliations: Holly E. Barker[1], Radhika Patel[1], Martin McLaughlin[1], Ulrike Schick[1,3], Shane Zaidi[1,2], Chris Nutting[2], Kate Newbold[2], Shreerang Bhide[1,2], Kevin Harrington[1,2]

[1]Targeted Therapy Team, Division of Cancer Biology, The Institute of Cancer Research, Chester Beatty Laboratories, London, United Kingdom, [2]Head and Neck Unit, The Royal Marsden NHS Foundation Trust, London and Surrey, United Kingdom, [3]Radiation Oncology Unit, University Hospital, Brest, France.

Running title: CHK1 inhibition chemoradiosensitises HNSCC cells

Key words: Head and neck cancer (HNSCC), CHK1 inhibition, paclitaxel, radiosensitisation, human papilloma virus (HPV)

Corresponding author: Holly E. Barker, The Institute of Cancer Research, Chester Beatty Laboratories, 237 Fulham Rd, London, SW3 6JB, United Kingdom, Tel: +44 (0) 207153-5150, Fax: +44 (0) 207352-5630, Email: holly.barker@icr.ac.uk

Conflict of interest: The authors have declared that no conflict of interest exists.

Manuscript: The manuscript is 4985 words with 6 figures and 40 references.

Abstract

Head and neck squamous cell carcinoma (HNSCC) is a leading cause of cancer-related deaths, with increasingly more cases arising due to high-risk human papillomavirus (HPV) infection. Cisplatin-based chemoradiotherapy is a standard-of-care for locally-advanced head and neck cancer, but is frequently ineffective. Research into enhancing radiation responses as a means of improving treatment outcomes represents a high priority. Here, we evaluated a CHK1 inhibitor (CCT244747) as a radiosensitiser and investigated whether a mechanistically rational triple combination of radiation/paclitaxel/CHK1 inhibitor delivered according to an optimised schedule would provide added benefit. CCT244747 abrogated radiation-induced G2 arrest in the p53-deficient HNSCC cell lines, HN4 and HN5, causing cells to enter mitosis with unrepaired DNA damage. The addition of paclitaxel further increased cell kill and significantly reduced tumour growth in an HN5 xenograft model. Triple therapy was shown to reduce the expression of several markers of radioresistance. Moreover, the more radioresistant HN5 cell line, which had high CHK1 activation following exposure to radiation, exhibited increased sensitivity to triple therapy than the more radiosensitive HN4 cells. We analysed CHK1 expression in a panel of head and neck tumours and observed that primary tumours from HPV+ patients, who went on to recur post-radiotherapy, exhibited significantly stronger expression of total and activated CHK1. CHK1 may serve as a biomarker to identify tumours likely to recur and, therefore, the patients who may benefit from concomitant treatment with a CHK1 inhibitor and paclitaxel during radiotherapy. Clinical translation of this strategy is under development.

Introduction

Head and neck squamous cell carcinoma (HNSCC) is the sixth leading cancer worldwide(1), with smoking, alcohol consumption, and high-risk human

papillomavirus (HPV) infection being the most common risk factors(2-4). Radiation therapy is a standard-of-care treatment for patients with HNSCC. Tumours of the same size and stage, however, may respond variably to radiation and new approaches to overcoming radioresistance and preventing tumour recurrence are continually being sought. Ionising radiation induces a DNA damage response (DDR) that involves the cooperation of a complex network of proteins, which play roles in cell cycle checkpoints and DNA repair(5). In normal cells, radiation-induced DNA damage predominantly induces a G1/S cell cycle arrest as a result of p53 activation. This G1/S checkpoint is typically lost in cancer cells, most often due to p53 loss, mutation, or inactivation (i.e. following human papillomavirus (HPV) infection) or disruption of p53-regulated processes(6). These cells, therefore, depend heavily on the S or G2/M cell cycle checkpoints to repair DNA damage following ionising radiation, a dependency which can be exploited therapeutically(7).

Ataxia telangiectasia and Rad3-related (ATR) and Ataxia telangiectasia mutated (ATM) are the initial DDR kinases activated by the sensors of DNA damage and, in turn, activate the downstream checkpoint effector kinases CHK1 and CHK2(8). One consequence of CHK1 activation is inhibition of the phosphatase CDC25C and subsequent arrest of cells in the G2/M phase of the cell cycle. CHK1 activity has also been shown to play a role in the G1/S, intra-S and mitotic spindle checkpoints, indicating that CHK1 is a fundamental component of the DDR and represents an ideal target for therapeutic intervention(9). We, and others, have shown that CHK1 inhibitors can enhance radiation cytotoxicity in cancer cells (reviewed in (7)). In the presence of CHK1 inhibitors, cells will attempt to undergo mitosis despite harbouring radiation-induced DNA damage. This can lead to chromosomal missegregation or loss of chromatid fragments, resulting in abnormal cell division and cell death in a process called mitotic catastrophe(10).

Patients with locally-advanced HNSCC typically receive cisplatin-based chemoradiotherapy (CCRT) but this is frequently ineffective and associated with severe acute and late toxicities(11). Therefore, alternative approaches to CCRT for HNSCC need to be developed. Taxanes are potent radiosensitisers and have been shown to be tolerable and active in combination with radiotherapy in patients with HNSCC(12). Since they disrupt normal mitotic progression, they represent attractive agents to combine with radiation and radiosensitisers that target the G2/M phase of the cell cycle (eg CHK1 inhibitors).

CCT244747 is a selective and orally bioavailable CHK1 inhibitor, which has previously been shown to enhance the anti-tumour activity of several genotoxic agents(13). Here, we investigated whether including paclitaxel provided added benefit to CCT244747 and radiation combination therapy and defined the schedule-dependence of the combined therapy. We also investigated possible biomarkers of radiation resistance and assessed the potential for this triple combination therapy in overcoming radiation resistance in head and neck cancer patients.

Materials and Methods

Cell lines

HN4 and HN5 human HNSCC cell lines were kindly provided by Sue Eccles (The Institute of Cancer Research, Sutton, UK). Cells were grown in Dulbecco's modified Eagle's medium (DMEM) supplemented with 5% foetal calf serum (FCS), 1% glutamine and 0.5% penicillin/streptomycin (ICR, London, UK). Cells were maintained at 37°C and 5% CO_2 in a humidified incubator, routinely tested for mycoplasma, and authenticated by short tandem repeat (STR) analysis within the last 6 months.

Drug preparation and irradiation

The CHK1 inhibitor CCT244747 was manufactured at the ICR (Sutton, UK). CCT244747 was dissolved in DMSO for *in vitro* experiments and in 10% DMSO, 5% Tween-80, 20% PEG400 and 65% H_2O for *in vivo* experiments. Paclitaxel was obtained from the Royal Marsden Hospital (London, UK). Irradiation was carried out using an AGO HS MP1 X-ray machine (AGO X-ray Limited, UK) at 250 kV and a dose rate of approximately 0.6 Gy/min.

MTT assays

Cells were plated in 96-well plates, treated with increasing concentrations of CCT244747 or paclitaxel, and cell viability assessed 72 hours later using the MTT (3-(4,5-dimethylthiazol-2-yl)-2,5-diphenyltetrazolium bromide; Sigma) assay according to manufacturer's instructions. Absorbance was measured at 550 nm on a SpectraMax M5 plate reader (Molecular Devices).

Flow cytometric analysis of cell cycle

Cells were treated with IC_{50} concentrations of CCT244747, paclitaxel, and/or 4 Gy radiation. Cells were trypsinised and fixed in 80% ethanol. For cell cycle analysis, cells were washed and resuspended in propidium iodide (PI) solution (20μg/mL PI and 100μg/mL RNase A; Sigma-Aldrich), incubated at 37°C for 30 minutes and analysed on a BD LSRII Flow Cytometer (BD Biosciences). To quantify the mitotic population, cells were blocked with 1% BSA and then incubated with phospho-Ser10 histone H3 (p-HH3) antibody conjugated to Alexa Fluor®-647 (Cell Signalling).

Western blotting

Lysates were prepared in RIPA buffer (50mM Tris; pH7.5, 150mM NaCl, 1% NP40, 0.5% sodium deoxycholate, 0.1% SDS) supplemented with a complete mini protease inhibitor cocktail tablet (Roche), 200μM sodium fluoride and 200μM sodium vanadate. Proteins were separated on Criterion™ TGX™ precast gels (Biorad). Gels were transferred onto Trans-Blot® Turbo™ Midi PVDF membranes using the Trans-Blot® Turbo™ Transfer system (Biorad). Membranes were probed with the following antibodies: phospho-S345 CHK1 (p-CHK1), CHK1, phospho-Thr68 CHK2 (p-CHK2), CHK2, phospho-Ser1981 ATM (p-ATM), ATM, phospho-S139 histone H2AX (γ-H2AX), Cyclin A2, Cyclin B1, MCL1, Caspase-3 (Cell Signalling, MA, USA), p-HH3 (Millipore), PARP (Santa Cruz), or β-actin (Abcam).

Clonogenic assays

For radiosensitisation studies, cells were treated with DMSO (vehicle control) or CCT244747 and irradiated with 1, 2 or 4 Gy one hour after drug or vehicle exposure. CCT244747 was washed off after 48 hours. After 10-14 days, colonies were fixed and stained with 5% gluteraldehyde, 0.5% crystal violet solution and counted. Surviving fractions (SF) were calculated by normalising for CCT244747 treatment. For triple combination studies, cells were treated with DMSO, CCT244747, paclitaxel and/or 2 Gy radiation according to schedule 1 or schedule 2.

Synergy assays

Cells were treated with 0.25x, 0.5x, 1x, 2x, and 4x IC_{50} concentrations of CCT244747 or paclitaxel or both, and cell viability assessed 72 hours later using MTT assay. Cell viability was calculated by comparing to vehicle-treated cells. Synergy was determined using the Bliss Independence Model, defined by equation $E_{exp} = E_x + E_y - (E_x E_y)$ where E_{exp} is the expected effect if the two drugs are additive and E_x and E_y are effects of the individual drugs(14). The equation $\Delta E = E_{obs} - E_{exp}$

6

is then used to ascertain synergy. If ΔE and the 95% CI values are all greater than 0, the two drugs demonstrate synergy.

In vivo experiments

HN5 cells were injected subcutaneously in female 6-8 week-old NOD *scid* gamma mice (NSG, JAX® Mice, Maine, USA). Once tumours had reached approximately 100mm^3, animals were divided into 8 treatment groups (8-12 mice per group). Treatment was given 3 times on alternate days. Mice received CCT244747 (125mg/kg) by oral gavage, paclitaxel (5mg/kg) by intraperitoneal injection and/or 2 Gy RT according to schedule 2. Tumour volume was obtained using the formula: Volume = Width x Length x Depth x 0.524mm^3. Mice were culled when tumours reached a maximum diameter of 15mm in one dimension. All animal studies were conducted in accordance with National Cancer Research Institute (NCRI) guidelines(15). All animal research was reviewed and approved by the Institute of Cancer Research Ethics Committee. These experiments were performed under the authority given by UK Home Office Project License PPL 70/7947.

Immunocytochemistry for DNA damage and nuclear morphology

Cells were treated with CCT244747, paclitaxel and/or 4 Gy radiation according to schedule 2. Cells were fixed with 4% paraformaldehyde, blocked with blocking buffer (1% BSA, 2% FCS) and incubated with rabbit anti-γ-H2AX (Cell signalling) and mouse anti-α-tubulin (Sigma-Aldrich) antibodies. Anti-rabbit 488 and anti-mouse 633 Alexa Fluor® secondary antibodies were used (Invitrogen, Molecular Probes™). Nuclei were counterstained with 4',6-diamidino-2-phenylindole dihydrochloride (DAPI; Invitrogen, Molecular Probes™). Cells were imaged using a LSM 710 inverse laser scanning microscope (Zeiss) and captured with a LSM T-PMT detector (Zeiss).

At least 275 cells from 5 fields of view and 3 independent experiments were counted. Cells with ≥5 γ–H2AX foci/nucleus were scored as positive.

Long-term growth assays

Cells were treated with CCT244747, paclitaxel and/or 4 Gy radiation according to schedule 2. Cells were trypsinised at 96, 168 and 336 hours and counted. Before trypsinisation at 336 hours, cells were imaged using an Eclipse TS100 microscope (Nikon) and images captured using a Digital Sight DS-L1 camera (Nikon).

Apoptosis Array

Cells were treated with vehicle or triple therapy according to schedule 2 and lysed after 48 hours in RIPA buffer. Membranes from a Human Apoptosis Array Kit (R&D Systems™) were incubated with prepared cell lysates and developed as per manufacturer's instruction. Dot intensity was calculated using ImageJ software (NIH, MD, USA).

Patient samples and immunohistochemistry

The PREDICTR-HNC study was approved by the Coventry Research Ethics Committee (reference number 10/H1210/9). Patient samples were collected at the Royal Marsden Hospital (London, UK). All tumours were of oropharynx origin. Biopsies were taken before patients received varying doses of radiotherapy with or without neoadjuvant chemotherapy. See Supplementary Table S1 for full tumour and therapy details. Immunohistochemistry was carried out on sections using the EnVision™ FLEX System (Dako) and antibodies specific for phospho-S345 CHK1 (p-CHK1) (Thermo Fisher Scientific), CHK1, phospho-Ser1981 ATM (p-ATM) (Abcam), Survivin (Dako) and Ki67 (Leica Biosystems). Sections were scanned

using an Ariol SL50 slide scanner and BX61 microscope (Olympus) and images captured using a U-CMAD3 camera (Olympus).

Statistical Analysis

Data were analysed using the Student t-test and considered significant when the *P* value was <0.05. All statistical tests were two-sided. Bar graphs represent the mean and standard error across at least 3 independent experimental repeats. Statistical significance representations: *, *P* < 0.05; **, *P* < 0.01; ***, *P* < 0.001; and ****, *P* < 0.0001.

Results

CHK1 inhibition radiosensitises HN4 and HN5 cells

To test the effect of inhibiting CHK1 on radiation-mediated G2 arrest, cells were treated with the CHK1 inhibitor, CCT244747, one hour before irradiation and then collected at indicated time-points. Mitotic cells were identified by phospho-Ser10 histone H3 (p-HH3) staining and flow cytometry. IC_{50} concentrations were calculated for CCT244747 (1μM for HN4 cells and 0.4μM for HN5 cells) and were used for subsequent experiments unless otherwise stated (Supplementary Figure S1A). As expected, radiation reduced the percentage of cells entering mitosis, suggesting that cells were arrested at the G2-phase of the cell cycle (Figure 1A). CCT244747 administration significantly abrogated the radiation-mediated reduction of mitotic HN4 and HN5 cells at 4 and 8 hours after 4 Gy (Figure 1A). We and others have previously shown that phospho-S345 CHK1 is the most consistent pharmacodynamic biomarker of CHK1 inhibition(16, 17). Western analysis confirmed CCT244747 drug-on-target activity as demonstrated by p-CHK1 expression (Figure 1B). p-HH3 expression was reduced in cells following irradiation as before, whereas cells pre-treated with CCT244747 had higher levels of p-HH3

expression at 4 and 8 hours after irradiation (Figure 1B), similar to results obtained using flow cytometry. Ionising radiation induces DNA double-strand breaks (DSBs), which result in rapid phosphorylation of histone H2AX at Ser139 (γ–H2AX). The presence of DNA DSBs in HN4 and HN5 cells following irradiation was determined by expression of γ-H2AX. Continued cell cycling after irradiation, due to CCT244747 treatment, resulted in the maintenance of DNA DSBs as shown by increased γ-H2AX expression, most notably at 12, 24 and 48 hours after irradiation in both cell lines. Importantly, CCT244747 pre-treatment led to significant radiosensitisation of HN4 and HN5 cells in clonogenic assays (Figure 1C and Supplementary Figure S1B).

CHK1 inhibition reduces paclitaxel-mediated mitotic arrest, but the combination is not synergistic in HN4 and HN5 cells

To test the effect of combining CCT244747 with paclitaxel on the mitotic population, cells were treated with CCT244747 one hour before paclitaxel treatment and then collected at indicated time-points for quantification of p-HH3 expressing cells by flow cytometry. IC_{50} concentrations were determined for paclitaxel using MTT assays (8nM for HN4 cells and 4nM for HN5 cells) and were used for subsequent experiments unless otherwise stated (Supplementary Figure S1A). Paclitaxel treatment increased the percentage of HN4 and HN5 cells in mitosis up to 24 hours (Figure 1D). When cells were pre-treated with CCT244747, accumulation in mitosis was initially unaffected, however, after 12 hours the mitotic population was significantly reduced in both cells lines (P=0.01 and 0.014 for HN4 and HN5 cells, respectively)(Figure 1D). Western analysis confirmed CCT244747 drug-on-target activity as demonstrated by accumulation of p-CHK1 expression (Figure 1E). p-HH3 expression was reduced slightly after 12 hours in cells pre-treated with CCT244747 compared to those treated with paclitaxel alone, however, a p-HH3 reduction was

most pronounced at 24 hours. Although the Western blotting and flow cytometry results vary slightly (possibly due to the sensitivities of the different antibodies used), both methods indicate that CHK1 inhibition enables cells to prematurely escape a paclitaxel-induced mitotic arrest. Moreover, CCT244747 pre-treatment results in increased DNA DSBs, demonstrated by increased expression of γ-H2AX, at 24 hours in both cells lines (Figure 1E). MTT assays were carried out to determine whether CCT244747 and paclitaxel acted synergistically. HN4 and HN5 cells were treated with varying ratios of IC_{50} concentrations of CCT244747 and paclitaxel independently or in combination and cell viability calculated relative to vehicle (DMSO) treated cells (Figure 1F). Bliss analysis of the MTT studies indicated that CCT244747 and paclitaxel only behaved synergistically in HN5 cells at a concentration of 0.5 x IC_{50} (Figure 1G).

A schedule for CCT244747, paclitaxel and radiation triple therapy synergistically kills HN4 and HN5 cells

We hypothesised that cells prematurely entering mitosis with radiation-induced DNA damage, due to pre-treatment with the CHK1 inhibitor, could be subsequently exposed to paclitaxel resulting in greater cell kill. Flow cytometry results suggested that treatment with paclitaxel 4-8 hours after CCT244747/radiation double therapy would affect the maximum number of damaged cells entering mitosis (see Figure 1A). In contrast, flow cytometry revealed that irradiation of cells 4-8 hours after CCT244747/paclitaxel double therapy would target the greatest number of cells arrested in mitosis, the most radiosensitive phase of the cell cycle[18-20](see Figure 1D). Therefore, we tested 2 schedules where cells were treated with CCT244747 and then exposed to radiation before paclitaxel (Schedule 1) or vice versa (Schedule 2) over the same 6 hour therapeutic window (Figure 2A). The short-term maintenance of DNA damage was determined by Western blotting for γ-H2AX

expression. Triple therapy according to Schedule 2 resulted in a greater γ-H2AX signal at 24 hours in HN4 and HN5 cells compared to schedule 1 (Figure 2B). The concurrent γ-H2AX and p-HH3 expression suggests that mitosis is occurring despite unrepaired DNA DSBs being present. Therefore, cells are at significant risk of undergoing mitotic catastrophe. In long-term clonogenic assays, HN4 and HN5 cells were dosed with 0.5μM CCT244747 and 3nM paclitaxel and 2 Gy of radiation. The surviving fraction (SF) of cells treated with triple therapy was significantly lower than the SF of cells treated with CCT244747/radiation double therapy only in HN5 cells when using schedule 2 (P=0.031; Figure 2C). Normalising SF values for CCT244747 and paclitaxel treatment again demonstrated a significant decrease in SF after triple therapy compared to CCT244747/radiation double therapy in HN5 cells when schedule 2 was used (P=0.001; Figure 2D). Clonogenic assays carried out with lower concentrations of 0.2μM CCT244747 and 1nM paclitaxel with 2 Gy of radiation resulted in a significantly lower SF following triple therapy only when compared with paclitaxel/radiation double therapy in HN5 cells using schedule 2 (P=0.0002; Supplementary Figure S2A). Normalising for drug effect, a lower SF after triple therapy was only seen in HN5 cells using schedule 2 but this difference was not significant (Supplementary Figure S2B). We used the Bliss Independence Model to determine whether paclitaxel synergised with CCT244747/radiation double therapy. Synergy was only observed for schedule 2 at the high drug concentrations in HN5 cells (Figure 2E). Taking into account all of the results obtained for the two triple therapy schedules, schedule 2 was selected for further analysis.

Triple therapy reduces the growth rate of HN5 xenografts

To assess the efficacy of the triple therapy in vivo, HN5 cells were implanted subcutaneously in NSG mice and treated according to schedule 2 (Figure 3A). Relatively low doses of all agents were used to ensure effects of the combination

therapies would be apparent and to reduce toxicity in the combination groups. Radiotherapy was the only single agent to show a significant reduction in tumour growth compared to controls (P=0.0343). Triple therapy significantly decreased tumour growth compared to all double therapy treatment groups (P<0.0001 when comparing with CCT244747 double combinations and P=0.0008 when comparing with the paclitaxel/radiotherapy combination; Figure 3B). HN5 tumours appeared to be more sensitive to radiation in vivo than might have been expected from in vitro data, possibly due to the fractionated nature of the in vivo treatment regimen. Interestingly, combining CCT244747 or paclitaxel with radiation did not cause a significant reduction in tumour growth above what was seen for tumours treated with radiation alone. Three tumours from each group were collected 2 hours after the final treatment for pharmacodynamic analysis. Western blotting of lysates prepared from these tumours demonstrated that, in most cases, CCT244747 activity could be detected by expression of p-CHK1. Furthermore, CCT244747 caused an increase in the mitotic population within the tumours as assessed by p-HH3 staining (Figure 3C).

Cells treated with CCT244747, paclitaxel and radiation triple therapy undergo mitotic catastrophe

To assess the appearance of the nuclei in cells after triple therapy using schedule 2, treated cells were fixed at 24 and 48 hours and analysed by confocal microscopy. Cells were stained with γ-H2AX to visualise DNA DSBs, and DAPI and α-tubulin to visualise nuclei and microtubules, respectively. Both HN4 and HN5 cells exhibited increased γ-H2AX foci after radiation, pan-H2AX staining (whole nuclear γ–H2AX staining) after CCT244747 treatment (as has been previously reported[21]), and abnormal nuclei after paclitaxel treatment (Figure 4A). Cells were quantified according to 6 categories: normal nuclear appearance, γ-H2AX foci, pan-H2AX

staining, abnormal nuclear morphology (micronuclei and/or multinuclear), abnormal nuclear morphology with γ-H2AX foci, and abnormal nuclear morphology with pan-H2AX staining (Figure 4B). Forty-eight hours after triple therapy, very few of the remaining cells had normal nuclear appearance. The most common characteristic in triple-treated cells was abnormal nuclear morphology, which was observed in 44.3% of HN4 cells and 67.5% of HN5 cells. HN4 cells exhibited significantly more micronuclei following triple therapy compared to HN5 cells (P=0.001) and HN5 cells were significantly more likely to be multinuclear following triple therapy compared to HN4 cells (P=0.044; Figure 4C), indicating mitosis was aberrant in both cell lines. Pan-H2AX staining occurred in cells exposed to CCT244747 with 43.0% and 51.9% of HN4 and HN5 triple-treated cells exhibiting pan-H2AX staining 48 hours after triple therapy, respectively. Pan-H2AX staining has previously been linked to stalled replication (S phase arrest), as well as being an indicator of inappropriate mitotic entry of cells harbouring unrepaired DNA damage from replication stress or checkpoint inhibition(22, 23). We have previously observed by Western blotting that mitosis is occurring after triple therapy despite the presence of unresolved DNA DSBs (Figure 2B). In addition, flow cytometry revealed that there was a 2.2-fold and 2.7-fold increase in the S phase population of HN5 cells 24 and 48 hours after triple therapy, respectively (Supplementary Figure S3A). Both of these findings could account for the increased pan-H2AX staining observed.

Triple therapy induces apoptosis and reduces clonogenicity in surviving cells
Pan-H2AX staining may also be an early indicator of cells destined for apoptosis(24). To assess whether HN4 and HN5 cells were undergoing apoptosis, sub-G1 analysis and western blotting were carried out 48 hours after triple therapy. Flow cytometry revealed significantly more HN4 cells (19.9 ± 2.8%, compared to 6.1 ± 2.1% HN5 cells) were undergoing the late stages of apoptosis (as assessed by the

percentage of cells in sub-G1) 48 hours after triple therapy (*P*=0.016; Figure 5A). Western blotting confirmed that HN4 cells were dying by apoptosis by virtue of decreased expression of MCL1 and the appearance of PARP and Caspase 3 cleavage in lysates harvested from treated cells 48 hours after triple therapy (Figure 5B). Decreased MCL1 expression could not be detected by Western blotting in HN5 cell lysates 48 hours after triple therapy, and only faint bands representing PARP and Caspase 3 could be detected (Figure 5B).

To assess whether HN5 cells were recovering at later time-points following triple therapy, as very few appeared to be undergoing apoptosis at 48 hours, long-term growth assays were carried out. Neither HN4 nor HN5 cells appeared to recover up to 2 weeks following treatment (Figure 5C) and many of the cells that remained appeared large and flat, or small and apoptotic (Figure 5D). Assays for senescence and autophagy were carried out with negative results (data not shown). The expression of apoptotic markers and cell cycle proteins was assessed at later time-points (96 and 120 hours) following triple therapy. Western blotting revealed that HN5 cells appeared to undergo delayed apoptosis since PARP and Caspase 3 cleavage could be easily detected by 120 hours, despite constant expression of MCL1 (Figure 5E). HN4 cells continued to display reduced expression of MCL1 following triple therapy, as well as sustained PARP and Caspase 3 cleavage. Interestingly, CHK1 appeared to be reactivated 96 and 120 hours after triple therapy, more so in HN5 cells (demonstrated by p-CHK1 expression, as CCT244747 was washed off at 48 hours). Consequently, the expression of Cyclin A2 was reduced, most prominently at 120 hours, whereas decreased Cyclin B1 expression was not observed (Figure 5E), suggesting cells arrested in S phase. These results suggest reactivation of CHK1 occurs in triple therapy-treated cells after drug wash-off, due to the presence of persistent DNA damage. When damage

is too great, cells undergo apoptosis at this later stage, whereas surviving cells appear to express reduced levels of Cyclin A2 and lose their clonogenicity.

Triple therapy reduces the expression of markers of radiation resistance

To further study changes in protein expression in HN4 and HN5 cells following triple therapy we used an apoptosis array. Cells were treated with triple therapy according to schedule 2 and lysates collected after 48 hours were used to probe an apoptosis array. The fold change in expression was calculated by comparing intensity of blots probed with lysate from treated cells with blots probed with lysates from vehicle-treated cells and converted to Log2 values (Supplementary Figure S4A). The expression of a number of proteins was decreased by at least half (<-1 on Log2 scale) in at least one cell line (Figure 6A). The expression of cleaved Caspase 3 was increased 3.1-fold and 1.6-fold in HN4 and HN5 cells, respectively, correlating with our previous western blots (Figure 5B). The expression of Claspin, a CHK1 adaptor protein, which undergoes proteasomal degradation during apoptosis, was decreased 9.0-fold and 4.0-fold in HN4 and HN5 cells, respectively, further confirming treatment efficacy. In addition to these findings, the expression of a number of proteins previously implicated in radiation resistance was reduced following triple therapy. Expression of the inhibitor of apoptosis proteins Survivin and XIAP was reduced 4.0-fold and 2.1-fold, respectively, in HN4 cells and 2.9-fold and 3.1-fold, respectively, in HN5 cells. We confirmed by Western blotting that down-regulation of Survivin and XIAP persisted at least 120 hours after triple therapy (Figure 6B).

CHK1 expression and activity as markers of radiation resistance

During this study, we noted that, despite HN5 cells being more resistant to radiation than HN4 cells, they appeared to be more sensitive to triple therapy. To investigate

the DDR pathways activated in HN4 and HN5 cells in response to radiation, cells were treated with 10 Gy and collected at specific time-points for analysis. DDR pathway activation was analysed in prepared lysates by Western blotting for phospho-S1981 ATM (p-ATM), p-CHK1 and phospho-T68 CHK2 (p-CHK2). p-HH3 expression confirmed that radiation-mediated G2 arrest occurred within 2 hours and was maintained at least until 6 hours (Figure 6C). HN4 cells had increased activation of CHK2 protein (p-CHK2 expression), whereas HN5 cells had strong CHK1 activation (p-CHK1 expression; Figure 6C). To determine whether CHK1 expression levels and activity could be a marker of resistance to radiotherapy, we analysed a panel of HPV+ and HPV- head and neck tumours by immunohistochemistry. Interestingly, high expression of total nuclear CHK1 protein as well as increased nuclear p-CHK1 expression significantly correlated with HPV+ tumours that recurred following radiotherapy (P=0.005, Figure 6D+E, Supplementary Figure S5). We noted that high cytoplasmic expression of CHK1 and p-CHK1 also significantly correlated with recurring HPV+ tumours (P=0.005 and 0.016, respectively; Supplementary Figure S4B+S5). We also analysed the expression of p-ATM, Ki67 and Survivin in these tumours. High expression of p-ATM was associated with recurring HPV+ tumours and low expression of Survivin was associated with non-recurring HPV+ tumours, however neither association was significant (P=0.078 and 0.053, respectively; Supplementary Figure S4C+S5). No correlation was observed between Ki67 expression levels and tumour recurrence.

Discussion

Detailed in vitro studies have been conducted to assess the efficacy of a range of CHK1 inhibitors in radiosensitising cancer cells that rely on the G2/M checkpoint for DNA damage repair(7). However, CHK1 inhibitors have not yet been combined with radiotherapy in clinical trials, possibly due to inadequate selectivity and/or

unexpected toxicities observed with earlier compounds(25, 26). The CHK1 inhibitor CCT244747 is a highly selective, potent, orally active ATP-competitive CHK1 inhibitor previously shown to enhance the activity of several genotoxic agents, including ionising radiation(13). The activity of CCT244747 has not previously been investigated in HNSCC cell lines. Here we confirmed that CCT244747 could overcome radiation-mediated G2 arrest in the p53-deficient HN4 and HN5 cells, causing cells to enter mitosis with unrepaired DNA damage. This led to significant radiosensitisation of both HN4 and HN5 cells in vitro.

We hypothesised that CCT244747 pre-treated p53-deficient cells entering mitosis harbouring radiation-mediated DNA damage could be further damaged with an antimitotic, such as paclitaxel. Indeed, greater cell kill was observed for triple therapy using this schedule (schedule 1). However, exploiting the ability of paclitaxel to arrest cells in mitosis, the most radiosensitive phase of the cell cycle, before exposing them to ionising radiation proved to be more effective (schedule 2). These findings reinforce the critical importance of optimising scheduling when combining different types of anticancer agents. Most importantly, including CCT244747 in our triple therapy enabled a much lower dose of paclitaxel to be used, therefore potentially limiting toxicity. Finally, administration of the triple therapy according to schedule 2 significantly reduced the growth rate of HN5 xenografts compared to all double combination therapies.

Cells receiving triple therapy exhibited many characteristics of mitotic catastrophe. The most common feature of cells exposed to triple therapy was the presence of nuclear abnormalities; cells often harboured micronuclei and/or were multinucleated. HN4 cells displayed more micronuclei, which could signal for them to be eliminated by apoptosis(27). Indeed, markers of apoptosis (namely an increased sub-G1

population, as well as Caspase 3 and PARP cleavage) were increased in HN4 cells 48 hours after triple therapy. HN5 cells, on the other hand, were more likely to be multinucleated following triple therapy. Cell cycle arrest was thought to be the primary response to multinucleation in HN5 cells, as the S phase population more than doubled after triple therapy. S phase arrest has also previously been associated with CHK1 activation and decreased expression of Cyclin A2(28). We hypothesised that reactivation of CHK1 (after drug wash-off) due to persisting DNA damage could lead to cell cycle arrest at later time-points. If cells are unable to repair DNA damage at this later stage, they may undergo delayed apoptosis. Indeed, markers of apoptosis could be detected 96 and 120 hours after triple therapy. Surviving cells appeared to have lost their clonogenicity and, as such, expressed decreased levels of the S phase regulator Cyclin A2.

Finally, we found that triple therapy reduced the expression of several markers of radiation resistance, including Survivin and XIAP, in both HN4 and HN5 cells. High expression of these proteins has previously been linked to radiation resistance and worse prognosis(29-32). During this study, it was noted that despite HN5 cells being highly radioresistant they were more sensitive to CCT244747 monotherapy, as well as CCT244747 combined therapies, than HN4 cells. Certainly, HN5 cells exhibited greater activation of CHK1 following irradiation, compared to HN4 cells. This correlates with findings from two recent studies carried out in non-small cell lung cancer where CHK1 levels and activity indicated sensitivity to therapy(33, 34). Likewise, we hypothesised that high CHK1 activity could be a marker of radiation resistance and may serve as a biomarker for tumours likely to relapse and, thus, identify the patients who would benefit the most from triple therapy. Analysis of a small panel of HPV+ and HPV- head and neck tumours revealed there was a significant correlation between high total CHK1 expression in the nucleus or

cytoplasm with recurrence after radiotherapy in HPV+ tumours. High p-CHK1 expression in the nucleus or cytoplasm also significantly correlated with recurring HPV+ tumours. While this is a small sample set, high CHK1 expression and/or activity has previously been correlated with therapy-resistant cancer cells(35, 36) and has been associated with high grade, high-risk tumours often resistant to therapy and poor prognosis(36-40). Confirmation of our findings in a larger head and neck cancer dataset will be required.

We propose that cells with high CHK1 proficiency, which resist the first round of treatment with chemotherapy or radiotherapy, will become dominant in a tumour and drive recurrence and relapse. Not only is it possible that CHK1 expression and activity will help identify those tumours associated with a worse prognosis, but also CHK1 is likely to continue being an important target for cancer treatment. The triple therapy we propose here; administration of a CHK1 inhibitor 1 hour prior to paclitaxel treatment and followed 6 hours later with radiotherapy, holds great promise for treating all tumours reliant on a G2 checkpoint for DNA damage repair but also for overcoming therapy resistance and hopefully preventing recurrence. The schedule that we have defined is highly compatible with current clinical practice in HNSCC. Biomarker driven clinical studies in patients with locally-advanced HNSCC represent a rapid and rational route to translating this strategy and offer a means of mitigating the severe toxicity associated with existing cisplatin-based chemoradiotherapy.

Author contributions

HEB designed the experiments, acquired the data, wrote and revised the manuscript. KH proposed and supervised the study. HEB, RP, MM, SZ and KH

analysed the data. US provided the clinical samples. All authors reviewed the results and edited the manuscript.

Acknowledgements

References

1.   Ferlay J, Shin HR, Bray F, Forman D, Mathers C, Parkin DM. Estimates of worldwide burden of cancer in 2008: GLOBOCAN 2008. Int J Cancer. 2010;127(12):2893-917.

2.   Chaturvedi AK, Anderson WF, Lortet-Tieulent J, Curado MP, Ferlay J, Franceschi S, et al. Worldwide trends in incidence rates for oral cavity and oropharyngeal cancers. J Clin Oncol. 2013;31(36):4550-9.

3.   Chaturvedi AK, Engels EA, Anderson WF, Gillison ML. Incidence trends for human papillomavirus-related and -unrelated oral squamous cell carcinomas in the United States. J Clin Oncol. 2008;26(4):612-9.

4.   Hashibe M, Brennan P, Benhamou S, Castellsague X, Chen C, Curado MP, et al. Alcohol drinking in never users of tobacco, cigarette smoking in never drinkers, and the risk of head and neck cancer: pooled analysis in the International Head and Neck Cancer Epidemiology Consortium. J Natl Cancer Inst. 2007;99(10):777-89.

5.   Jackson SP, Bartek J. The DNA-damage response in human biology and disease. Nature. 2009;461(7267):1071-8.

6.   Begg AC, Stewart FA, Vens C. Strategies to improve radiotherapy with targeted drugs. Nat Rev Cancer. 2011;11(4):239-53.

7.   Dillon MT, Good JS, Harrington KJ. Selective targeting of the G2/M cell cycle checkpoint to improve the therapeutic index of radiotherapy. Clin Oncol (R Coll Radiol). 2014;26(5):257-65.

8.   Stracker TH, Usui T, Petrini JH. Taking the time to make important decisions: the checkpoint effector kinases Chk1 and Chk2 and the DNA damage response. DNA Repair (Amst). 2009;8(9):1047-54.

9.   Dai Y, Grant S. New insights into checkpoint kinase 1 in the DNA damage response signaling network. Clin Cancer Res. 2010;16(2):376-83.

10.   Vitale I, Galluzzi L, Castedo M, Kroemer G. Mitotic catastrophe: a mechanism for avoiding genomic instability. Nat Rev Mol Cell Biol. 2011;12(6):385-92.

11.   Machtay M, Moughan J, Trotti A, Garden AS, Weber RS, Cooper JS, et al. Factors associated with severe late toxicity after concurrent chemoradiation for locally advanced head and neck cancer: an RTOG analysis. J Clin Oncol. 2008;26(21):3582-9.

12.   Behera M, Owonikoko TK, Kim S, Chen Z, Higgins K, Ramalingam SS, et al. Concurrent therapy with taxane versus non-taxane containing regimens in locally advanced squamous cell carcinomas of the head and neck (SCCHN): a systematic review. Oral Oncol. 2014;50(9):888-94.

13.   Walton MI, Eve PD, Hayes A, Valenti MR, De Haven Brandon AK, Box G, et al. CCT244747 is a novel potent and selective CHK1 inhibitor with oral efficacy alone and in combination with genotoxic anticancer drugs. Clin Cancer Res. 2012;18(20):5650-61.

14.   Greco WR, Bravo G, Parsons JC. The search for synergy: a critical review from a response surface perspective. Pharmacol Rev. 1995;47(2):331-85.

15.   Workman P, Aboagye EO, Balkwill F, Balmain A, Bruder G, Chaplin DJ, et al. Guidelines for the welfare and use of animals in cancer research. Br J Cancer. 2010;102(11):1555-77.

16.   Borst GR, McLaughlin M, Kyula JN, Neijenhuis S, Khan A, Good J, et al. Targeted radiosensitization by the Chk1 inhibitor SAR-020106. Int J Radiat Oncol Biol Phys. 2013;85(4):1110-8.

17.   Parsels LA, Qian Y, Tanska DM, Gross M, Zhao L, Hassan MC, et al. Assessment of chk1 phosphorylation as a pharmacodynamic biomarker of chk1 inhibition. Clin Cancer Res. 2011;17(11):3706-15.

18.   Chen Y, Pandya K, Keng PP, Feins R, Raubertas R, Smudzin T, et al. Schedule-dependent pulsed paclitaxel radiosensitization for thoracic malignancy. Am J Clin Oncol. 2001;24(5):432-7.

19.   Zanelli GD, Quaia M, Robieux I, Bujor L, Santarosa M, Favaro D, et al. Paclitaxel as a radiosensitiser: a proposed schedule of administration based on in vitro data and pharmacokinetic calculations. Eur J Cancer. 1997;33(3):486-92.

20.   Zhang H, Hyrien O, Pandya KJ, Keng PC, Chen Y. Tumor response kinetics after schedule-dependent paclitaxel chemoradiation treatment for inoperable non-small cell lung cancer: a model for low-dose chemotherapy radiosensitization. J Thorac Oncol. 2008;3(6):563-8.

21.   Syljuasen RG, Sorensen CS, Hansen LT, Fugger K, Lundin C, Johansson F, et al. Inhibition of human Chk1 causes increased initiation of DNA replication, phosphorylation of ATR targets, and DNA breakage. Mol Cell Biol. 2005;25(9):3553-62.

22.   Gagou ME, Zuazua-Villar P, Meuth M. Enhanced H2AX phosphorylation, DNA replication fork arrest, and cell death in the absence of Chk1. Mol Biol Cell. 2010;21(5):739-52.

23. Liu S, Opiyo SO, Manthey K, Glanzer JG, Ashley AK, Amerin C, et al. Distinct roles for DNA-PK, ATM and ATR in RPA phosphorylation and checkpoint activation in response to replication stress. Nucleic Acids Res. 2012;40(21):10780-94.

24. Solier S, Pommier Y. The nuclear gamma-H2AX apoptotic ring: implications for cancers and autoimmune diseases. Cell Mol Life Sci. 2014;71(12):2289-97.

25. Thompson R, Eastman A. The cancer therapeutic potential of Chk1 inhibitors: how mechanistic studies impact on clinical trial design. Br J Clin Pharmacol. 2013;76(3):358-69.

26. Ma CX, Janetka JW, Piwnica-Worms H. Death by releasing the breaks: CHK1 inhibitors as cancer therapeutics. Trends Mol Med. 2011;17(2):88-96.

27. Decordier I, Dillen L, Cundari E, Kirsch-Volders M. Elimination of micronucleated cells by apoptosis after treatment with inhibitors of microtubules. Mutagenesis. 2002;17(4):337-44.

28. Tu YS, Kang XL, Zhou JG, Lv XF, Tang YB, Guan YY. Involvement of Chk1-Cdc25A-cyclin A/CDK2 pathway in simvastatin induced S-phase cell cycle arrest and apoptosis in multiple myeloma cells. Eur J Pharmacol. 2011;670(2-3):356-64.

29. Fraunholz I, Rodel C, Distel L, Rave-Frank M, Kohler D, Falk S, et al. High survivin expression as a risk factor in patients with anal carcinoma treated with concurrent chemoradiotherapy. Radiat Oncol. 2012;7:88.

30. Rodel F, Hoffmann J, Distel L, Herrmann M, Noisternig T, Papadopoulos T, et al. Survivin as a radioresistance factor, and prognostic and therapeutic target for radiotherapy in rectal cancer. Cancer Res. 2005;65(11):4881-7.

31. Flanagan L, Kehoe J, Fay J, Bacon O, Lindner AU, Kay EW, et al. High levels of X-linked Inhibitor-of-Apoptosis Protein (XIAP) are indicative of radio chemotherapy resistance in rectal cancer. Radiat Oncol. 2015;10(1):131.

32.   Moussata D, Amara S, Siddeek B, Decaussin M, Hehlgans S, Paul-Bellon R, et al. XIAP as a radioresistance factor and prognostic marker for radiotherapy in human rectal adenocarcinoma. Am J Pathol. 2012;181(4):1271-8.

33.   Grabauskiene S, Bergeron EJ, Chen G, Chang AC, Lin J, Thomas DG, et al. CHK1 levels correlate with sensitization to pemetrexed by CHK1 inhibitors in non-small cell lung cancer cells. Lung Cancer. 2013;82(3):477-84.

34.   Grabauskiene S, Bergeron EJ, Chen G, Thomas DG, Giordano TJ, Beer DG, et al. Checkpoint kinase 1 protein expression indicates sensitization to therapy by checkpoint kinase 1 inhibition in non-small cell lung cancer. J Surg Res. 2014;187(1):6-13.

35.   Bao S, Wu Q, McLendon RE, Hao Y, Shi Q, Hjelmeland AB, et al. Glioma stem cells promote radioresistance by preferential activation of the DNA damage response. Nature. 2006;444(7120):756-60.

36.   Seol HJ, Yoo HY, Jin J, Joo KM, Kim HS, Yoon SJ, et al. The expression of DNA damage checkpoint proteins and prognostic implication in metastatic brain tumors. Oncol Res. 2011;19(8-9):381-90.

37.   Cole KA, Huggins J, Laquaglia M, Hulderman CE, Russell MR, Bosse K, et al. RNAi screen of the protein kinome identifies checkpoint kinase 1 (CHK1) as a therapeutic target in neuroblastoma. Proc Natl Acad Sci U S A. 2011;108(8):3336-41.

38.   Roe OD, Szulkin A, Anderssen E, Flatberg A, Sandeck H, Amundsen T, et al. Molecular resistance fingerprint of pemetrexed and platinum in a long-term survivor of mesothelioma. PLoS One. 2012;7(8):e40521.

39.   Yao H, Yang Z, Li Y. [Expression of checkpoint kinase 1 and polo-like kinase 1 and its clinicopathological significance in benign and malignant lesions of the stomach]. Zhong Nan Da Xue Xue Bao Yi Xue Ban. 2010;35(10):1080-4.

40.   Al-Kaabi MM, Alshareeda AT, Jerjees DA, Muftah AA, Green AR, Alsubhi NH, et al. Checkpoint kinase1 (CHK1) is an important biomarker in breast cancer having a role in chemotherapy response. Br J Cancer. 2015;112(5):901-11.

Figure Legends

Figure 1: The CHK1 inhibitor CCT244747 overcomes radiation-mediated G2 arrest and reduces paclitaxel-mediated mitotic arrest in HN4 and HN5 cells

(A) Quantification of mitotic cells following 4 Gy of radiation (RT) with or without CCT244747 (CCT) pre-treatment. Cells were fixed at indicated time-points, stained with phosho-S10 Histone H3 (p-HH3) and analysed by flow cytometry. Data expressed as fold changes (0 hour = 1). **(B)** Western blot analysis of CCT drug on target activity (accumulation of phospho-S345 CHK1), mitotic cells (expression of p-HH3), and sustained DNA DSBs (expression of γ-H2AX) after 4 Gy of RT with or without CCT pre-treatment. Expression of β-actin provided a loading control. **(C)** Analysis of CCT244747 mediated radiosensitisation using clonogenic assays. Cells were treated with 0.2 μM or 0.7 μM CCT one hour before exposure to indicated doses of RT and data normalised for drug effect. **(D)** Quantification of mitotic cells following exposure to PTX with or without CCT pre-treatment, as described in (A). **(E)** Western blot analysis of CCT drug on target activity, mitotic cells, and sustained DNA DSBs after exposure to PTX with or without CCT pre-treatment. Expression of β-actin provided a loading control. **(F)** Quantification of surviving fractions following CCT or PTX monotherapy, or combined treatment, at the indicated ratios of IC_{50} doses for CCT and PTX. Surviving cells were quantified using MTT assays. **(G)** Analysis of synergy using the Bliss Independence Model. The difference in observed and expected effects ($\Delta E = E_{obs} - E_{exp}$) indicates synergy when ΔE and the 95% CI values are all greater than 0. *, $P < 0.05$; **, $P < 0.01$; ***, $P < 0.001$; and ****, $P < 0.0001$.

Figure 2: Scheduling of CCT244747, paclitaxel and radiation triple therapy

(A) Schematic of the 2 schedules chosen for further analysis. **(B)** Western blot analysis of CCT244747 (CCT) drug on target (accumulation of p-CHK1), mitotic cells (expression of p-HH3) and sustained DNA DSBs (expression of γ-H2AX) 24 hours after triple therapy according to schedule 1 or 2. Expression of β-actin provided a loading control. **(C)** Quantification of cell survival after triple therapy using clonogenic assays. Cells were treated with vehicle, 0.5 μM CCT, 3 nM paclitaxel (PTX), and/or 2 Gy radiation (RT) according to schedule 1 or 2. Surviving fractions (SF) were calculated by comparing treated wells with control wells. **(D)** Quantification of the SF when normalising for drug effects. **(E)** Analysis of synergy using the Bliss Independence Model. The effect of triple therapy is compared with the effects of CCT and chemoradiotherapy (PTX+RT) independently. *, $P < 0.05$; **, $P < 0.01$; ***, $P < 0.001$; and ****, $P < 0.0001$.

Figure 3: Triple therapy significantly delays HN5 xenograft tumour growth

(A) Schematic of in vivo triple therapy schedule used for treatment of mice harbouring HN5 xenografts. **(B)** Tumour volume of HN5 xenografts after indicated therapies. Tumours were measured bi-weekly in three dimensions. Significance is only indicated between groups that differ by a single agent. **(C)** Western blot analysis of CCT244747 (CCT) drug on target activity (accumulation of p-CHK1) and drug effect (CCT, paclitaxel (PTX) and radiation (RT)) on the mitotic population (expression of p-HH3). Expression of β-actin provided a loading control. *, $P < 0.05$; **, $P < 0.01$; ***, $P < 0.001$; and ****, $P < 0.0001$.

Figure 4: HN4 and HN5 cells have abnormal nuclear appearance after triple therapy

(A) Confocal analysis of HN4 and HN5 cells treated with CCT244747 (CCT) 1 hour before treatment with paclitaxel (PTX) and 6 hours before 4 Gy of radiation (RT). Cells were fixed and stained with anti-γ-H2AX antibody (green) to detect sustained DNA DSBs. Cells were co-stained with anti-α-tubulin antibody (red) and counterstained with DAPI (blue) to distinguish nuclear morphology. Representative images from one experimental repeat of cells fixed and stained at 48 hours are shown. Scale bar = 50 μM. **(B)** Quantification of confocal data for HN4 and HN5 cells at 24 and 48 hours following triple therapy as described in (A). **(C)** Quantification of cells with micronuclei and multinuclei 48 hours after triple therapy as described in (A). *, $P < 0.05$; **, $P < 0.01$; ***, $P < 0.001$; and ****, $P < 0.0001$.

Figure 5: HN5 cells exhibit delayed apoptosis and loss of clonogenicity after triple therapy

(A) Quantification of cells in the sub-G1 population following indicated treatments according to schedule 2. Cells were fixed at 24 and 48 hours, stained with propidium iodide and analysed by flow cytometry. **(B)** Western blot analysis of cell lysates 48 hours after indicated treatments according to schedule 2. Induction of apoptosis was analysed by blotting for MCL1, PARP and Caspase 3. Expression of β-actin provided a loading control. **(C)** Long-term growth assays of treated cells. Drugs were washed off after 48 hours and cells counted at indicated time-points. **(D)** Representative images of cells remaining at the end of the long-term growth assays described in (A). Scale bar = 100 μM. **(E)** Western blot analysis of HN4 and HN5 cell lysates 96 and 120 hours after indicated treatments. Apoptosis was analysed by blotting for MCL1, PARP and Caspase 3. Cell cycle progression was analysed by blotting for Cyclin A2 and Cyclin B1. Expression of β-actin provided a loading control. *, $P < 0.05$; **, $P < 0.01$; ***, $P < 0.001$; and ****, $P < 0.0001$.

Figure 6: Triple therapy down-regulates markers of radiation resistance and high CHK1 expression and activity correlate with recurring HPV+ head and neck tumours

(A) Analysis of protein expression in HN4 and HN5 cells 48 hours after triple therapy according to schedule 2 using an apoptosis array. Proteins with greatest fold change (compared to untreated controls) shown. **(B)** Western blot analysis of cell lysates 120 hours after indicated treatments according to schedule 2. Findings from the apoptosis array described in (A) were confirmed by blotting for Survivin and XIAP. Expression of β-actin provided a loading control. **(C)** Western blot analysis of HN4 and HN5 cells following exposure to 10 Gy of radiation (RT). Checkpoint activity was determined by blotting for p-ATM, p-CHK1 and p-CHK2. The mitotic population was also analysed by blotting for p-HH3. Expression of β-actin provided a loading control. **(D)** Quantification of CHK1 nuclear staining by IHC in HPV+ and HPV- HNSCC samples obtained from patients in the PredictR-HNC trial. **(E)** Quantification of p-CHK1 nuclear staining in patient samples as described in (D). **, $P < 0.01$.

Figure 1

Figure 2

A

Schedule 1

CCT   RT   PTX

1   2   3   4   5   6

Schedule 2

CCT   PTX   RT

1   2   3   4   5   6

Hours

B

C

D

E

Figure 3

A

Schedule 2 therapy
given on alternate days

2 weeks

2×10^6 HN5
cells implanted

Tumours collected
for PD analysis

Tumour volumes
measured bi-weekly
from start of treatment
until maximum
volume reached
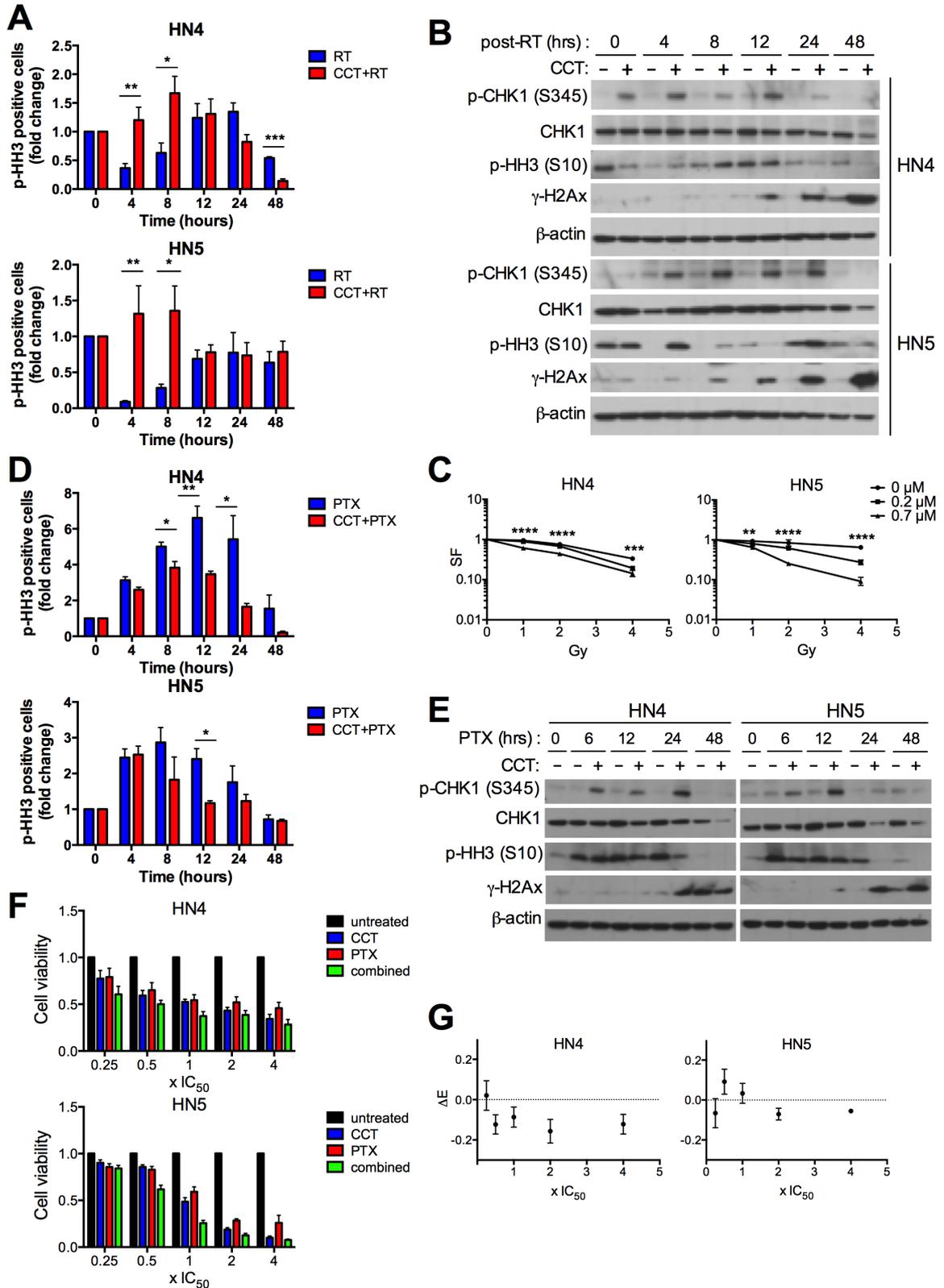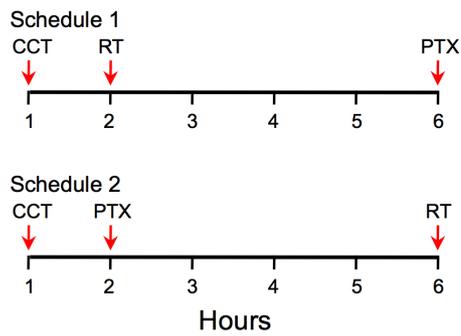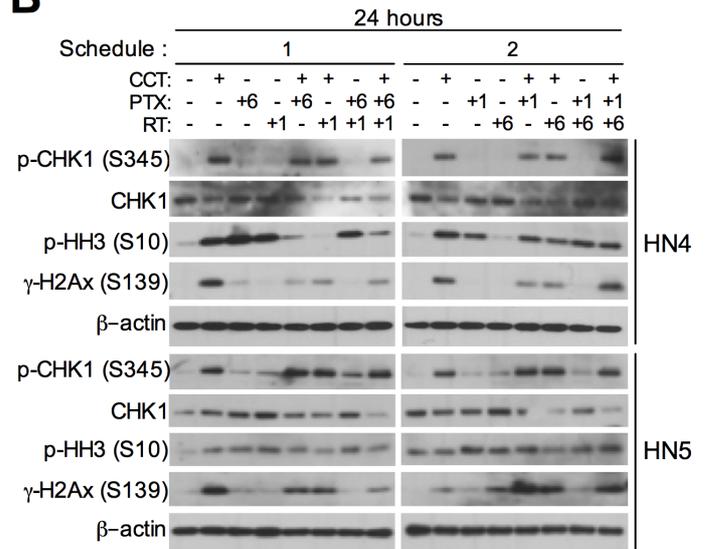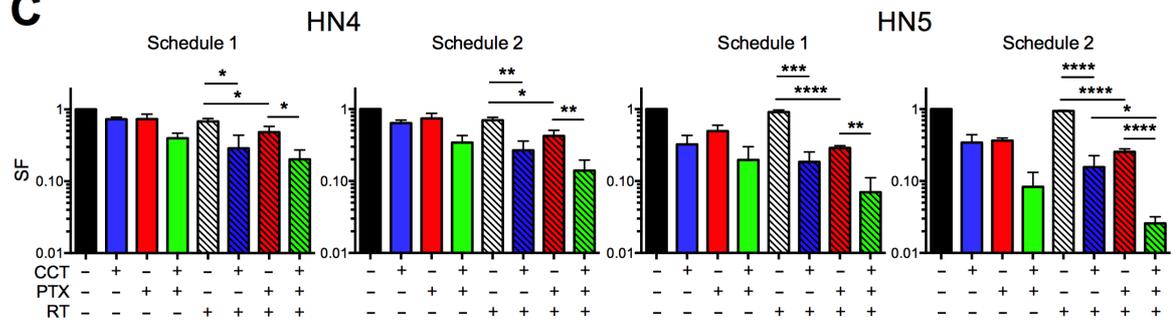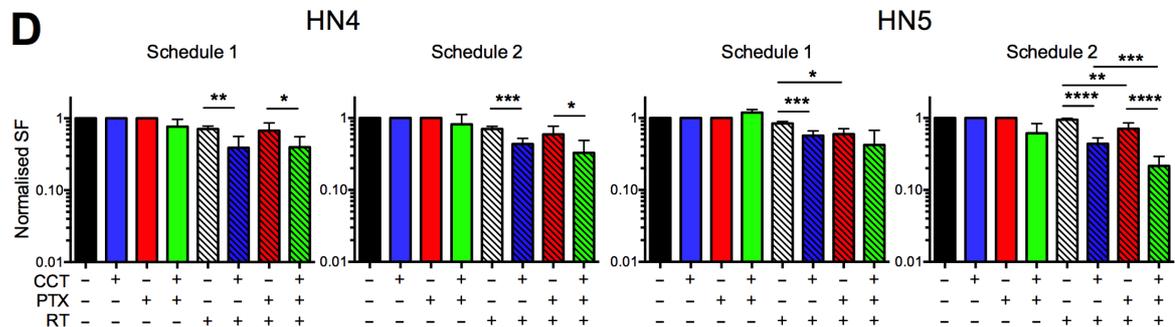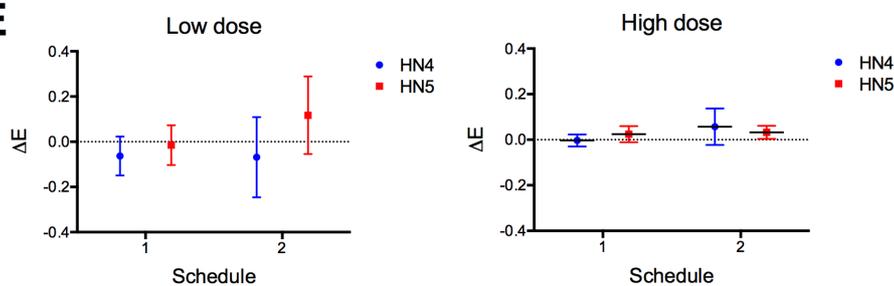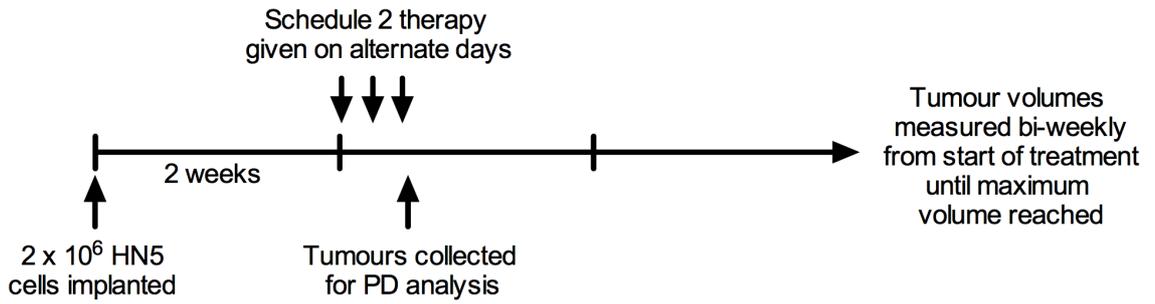
B

Absolute tumour volume

control
CCT
PTX
RT
CCT+PTX
CCT+RT
PTX+RT
CCT+PTX+RT

Tumour volume (mm^3)

Days after implantation

C

| Treatment: | cont | CCT | RT | CCT+RT | PTX | CCT+PTX | PTX+RT | CCT+PTX+RT |

p-CHK1 (S345)

CHK1

p-HH3

β−actin
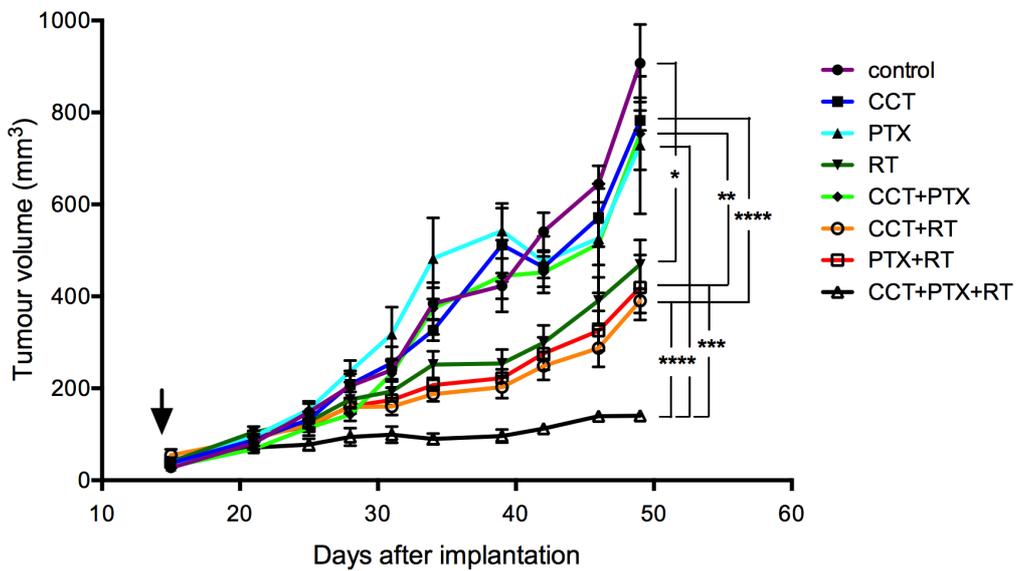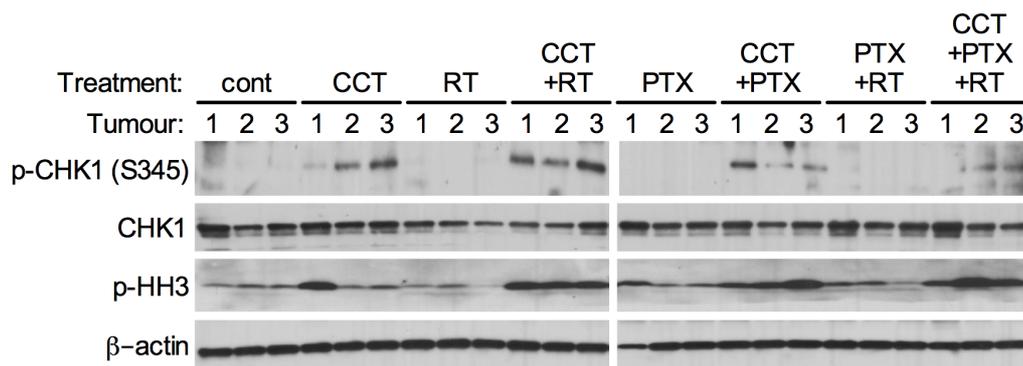
Figure 4

Figure 5

Figure 6

A

B

120 hours

C

D

CHK1 nuclear staining

E

p-CHK1 nuclear staining
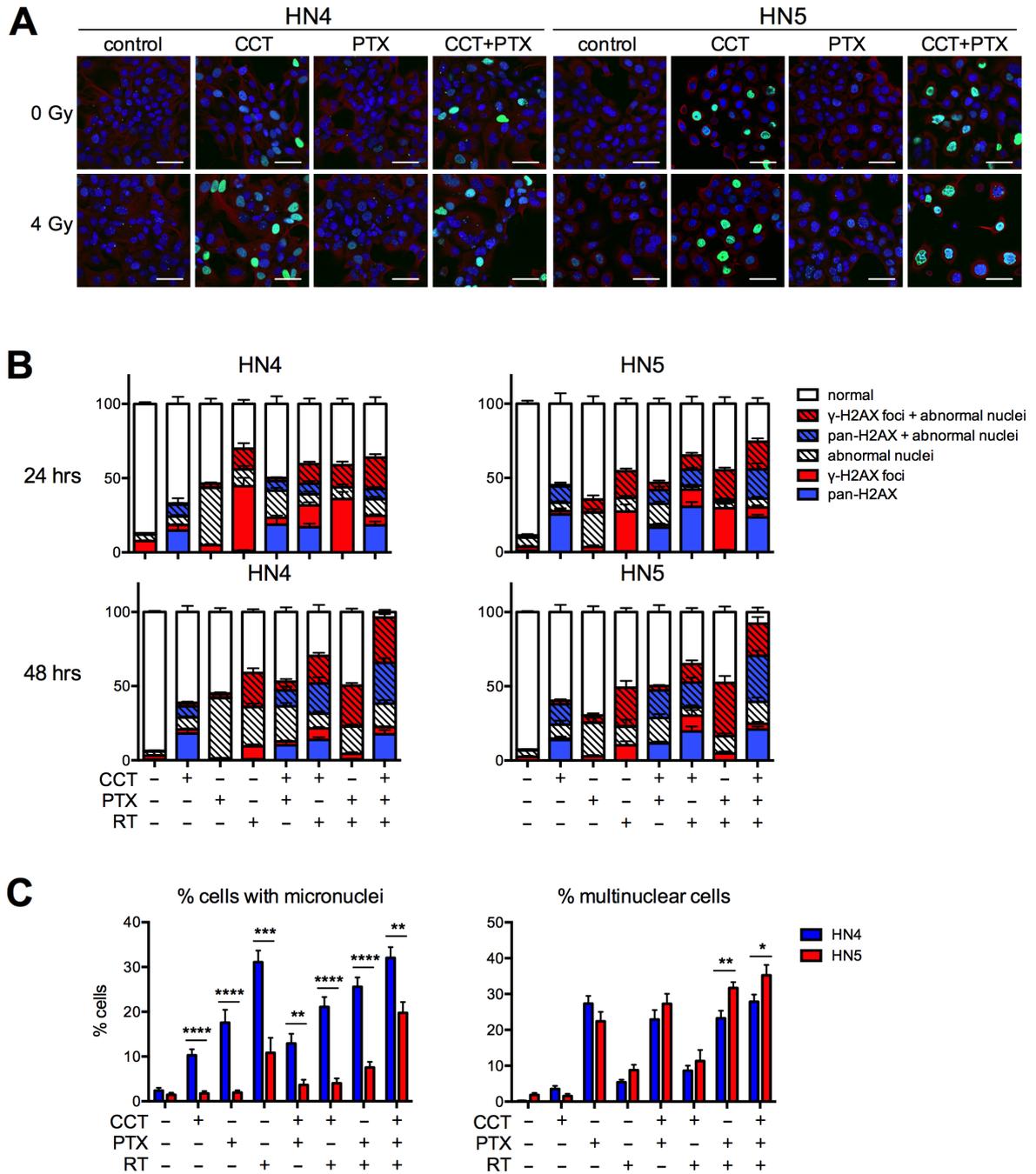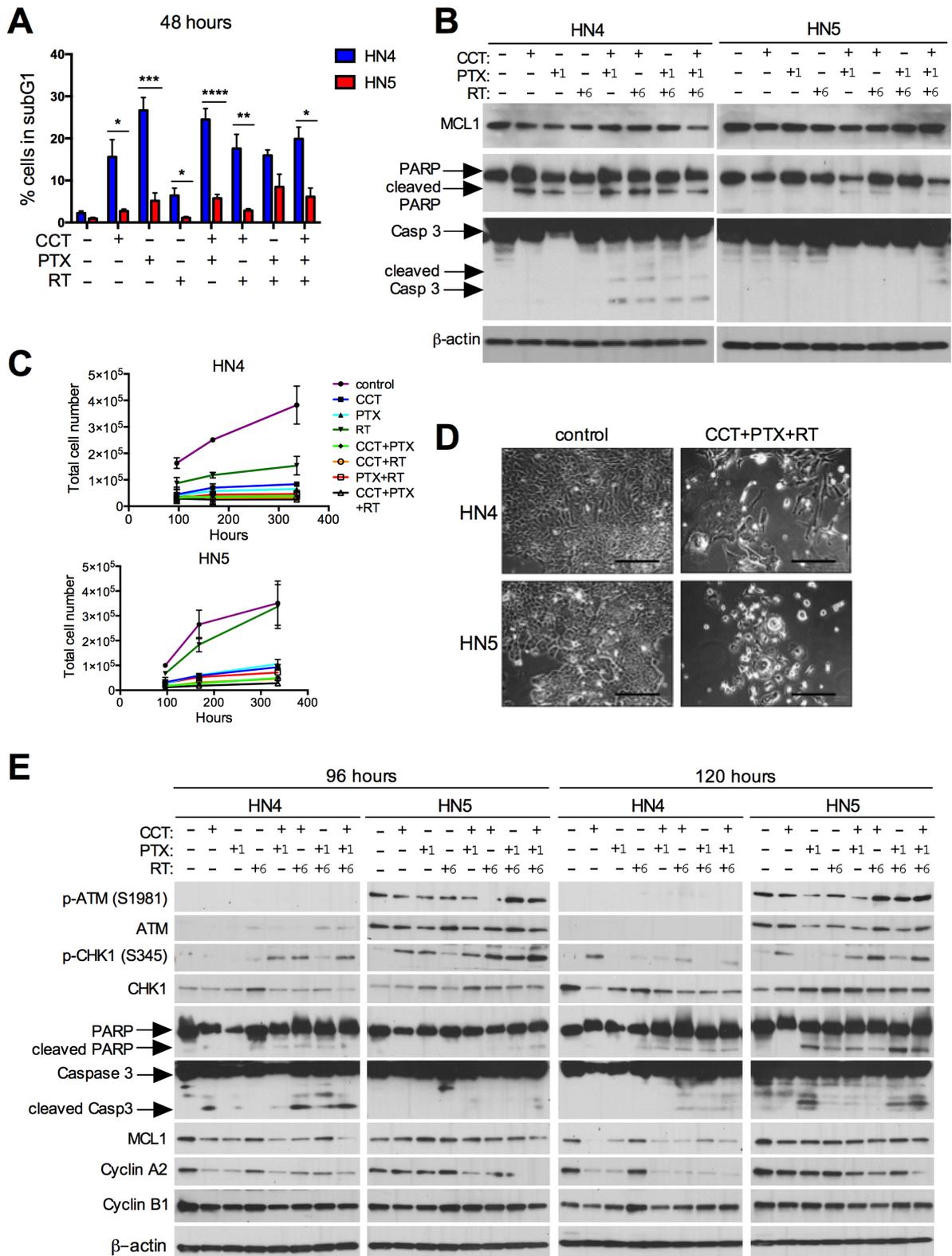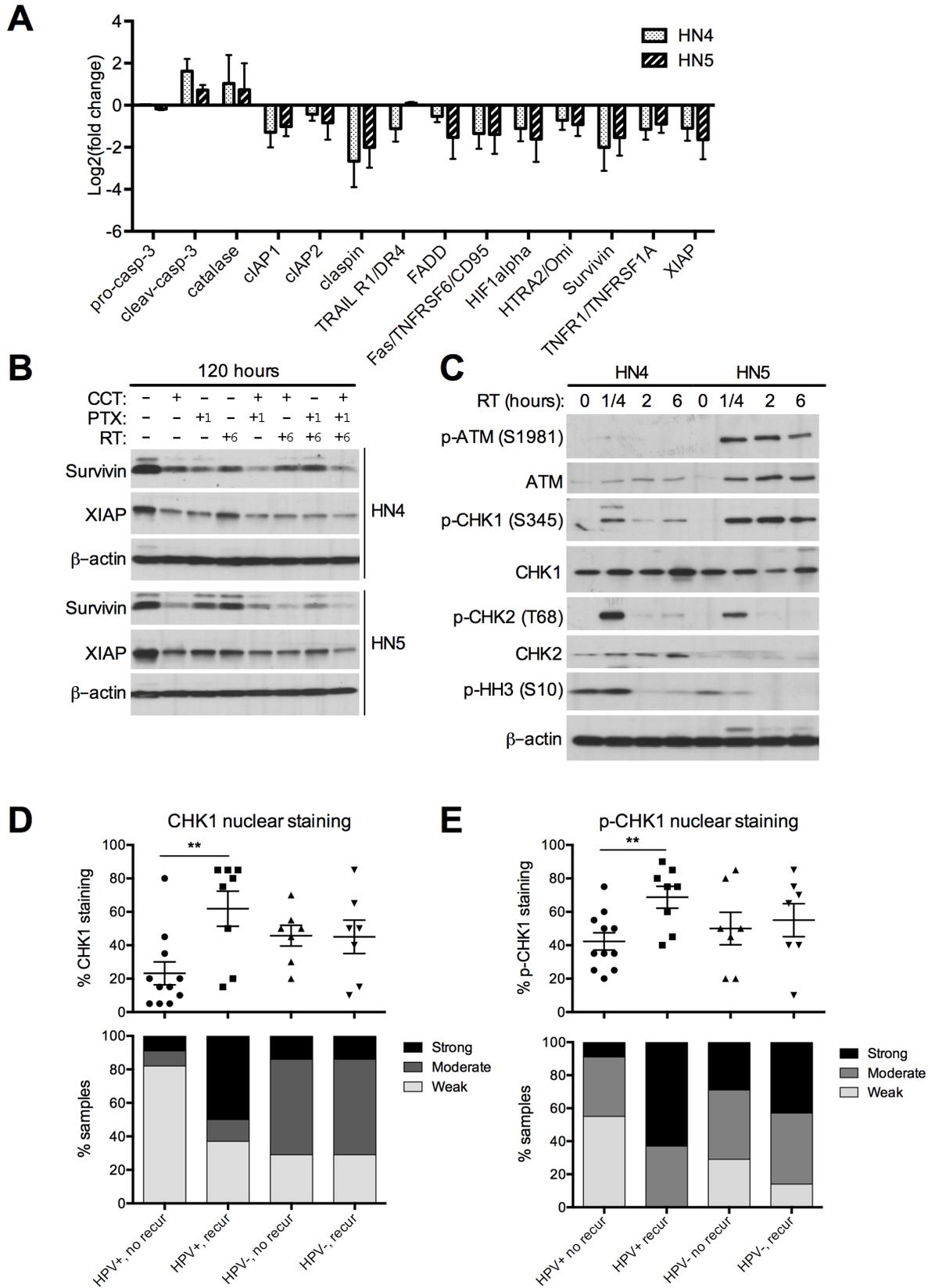
Supplementary Table S1: Patient samples from PredictR-HNC study

Tumours of the oropharynx collected from patients in the PredictR study. Patients received radiotherapy with or without chemotherapy. Tumour recurrence was noted out to at least 2 years. Patients without recurrence had been followed up 2 - 7.5 years after radiotherapy.

Patient sample #	T stage	N stage	M stage	HPV status	Recurrence 1 = yes 0 = no	RT Type 1 = primary 2 = adjuvant 3 = palliative	Chemotherapy 1 = none 2 = concomitant 3 = neoadjuvant 4 = neoadjuvant and concomitant
RMH 116	3	2b	0	+	1	1	3
RMH 120	3	2c	0	+	1	1	4
RMH 121	2	0	0	-	1	1	
RMH 122	4	1	0	-	1	1	4
RMH 132	0	2b	0	+	0	2	2
RMH 134	3	1	0	-	0	2	3
RMH 135	4	1	0	-	1	1	3
RMH 141	2	0	0	+	0	2	1
RMH 142	3	2c	0	+	0	1	3
RMH 146	2	2b	0	+	0	2	2
RMH 147	1	2b	0	+	0	2	2
RMH 149	4	2c	0	+	1	1	4
RMH 150	3	1	0	+	1	3	pall
RMH 151	3	0	0	-	0	1	4
RMH 154	2	0	0	+	0	1	1
RMH 155	3	2b	0	+	1	1	4
RMH 157	2	2a	0	+	0	1	2
RMH 159	2	2a	0	+	0	2	2
RMH 163	1	2b	0	+	0	1	4
RMH 164	1	2b	0	+	0	2	2
RMH 165	2	2c	0	+	1	1	1
RMH 167	2	1	0	+	0	2	2
RMH 172	3	2b	0	-	1	1	4
RMH 173	4	3	0	+	1	1	4
RMH 175	4	2b	0	+	1	1	4
RMH 176	2	2a	0	-	0	1	1
RMH 184	4	2b	0	-	0	1	4
RMH 187	2	0	0	-	0	1	1
RMH 190	2	0	0	-	0	1	1
RMH 195	2	2b	0	-	0	2	1
RMH 196	3	0	0	-	1	1	3
RMH 199	4	2b	0	-	1	1	4
RMH 209	4	0	0	-	1	1	2

Supplementary Figure Legends:

Supplementary Figure 1: CCT244747 and paclitaxel IC$_{50}$ determination and CCT244747 radiosensitisation

(A) Quantification of IC$_{50}$ values for CCT244747 (CCT) and paclitaxel (PTX) using MTT assays. Cells were treated with indicated concentrations of the drugs and cell survival measured after 72 hours. Surviving fractions (SF) were calculated by comparing to vehicle treated controls. **(B)** Representative images of clonogenic assays. Cells were treated with 0.2 μM or 0.7 μM CCT one hour before exposure to indicated doses of RT.

Supplementary Figure S2: Investigation of triple therapies using low concentrations of CCT244747 and paclitaxel

(A) Quantification of cell survival after triple therapy using clonogenic assays. Cells were treated with vehicle, 0.2 μM CCT244747 (CCT), 1 nM paclitaxel (PTX) and/or 2 Gy radiation (RT) according to schedule 1 or 2. Surviving fractions (SF) were calculated by comparing with control wells. **(B)** Quantification of the SF when normalising for drug effect. *, $P < 0.05$; **, $P < 0.01$; and ***, $P < 0.0001$.

Supplementary Figure S3: HN5 cells exhibit an early increase in the S phase population

(A) Quantification of the S phase population of cells following triple therapy according to schedule 2. Cells were fixed at 24 and 48 hours, stained with propidium iodide and analysed by flow cytometry. *, $P < 0.05$.

Supplementary Figure S4: High CHK1 and p-CHK1 cytoplasmic staining correlate with recurring HPV+ head and neck tumours

(A) Analysis of protein expression in HN4 and HN5 cells 48 hours after triple therapy according to schedule 2 using an apoptosis array. Fold changes were calculated by comparing to vehicle treated controls. **(B)** Quantification of CHK1 and p-CHK1 cytoplasmic staining by immunohistochemistry in HPV+ and HPV- HNSCC samples obtained from patients in the PredictR-HNC strudy. **(C)** Quantification of p-ATM, Ki67 and Survivin expression in tumour samples described in (B). *, $P < 0.05$; and **, $P < 0.01$.

Supplementary Figure S5: High CHK1 p-CHK1 and p-ATM expression correlate with non-recurring tumours

Representative images of tumour samples taken from HPV+ HNSCC patients in the PredictR-HNC study stained with CHK1, p-CHK1, p-ATM, Survivin and Ki67. Scale bar = 100 μM.

Supplementary Figure S1

A
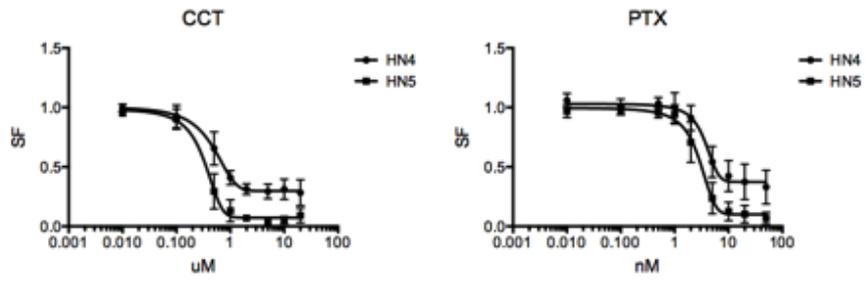
B

Supplementary Figure S2

A

HN4

HN5

B

HN4

HN5
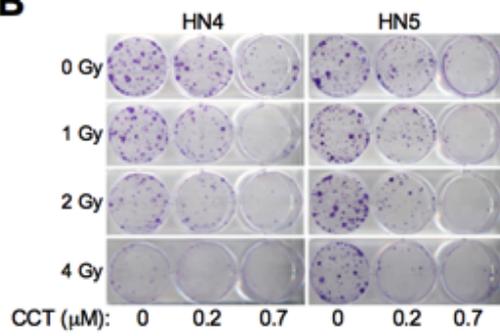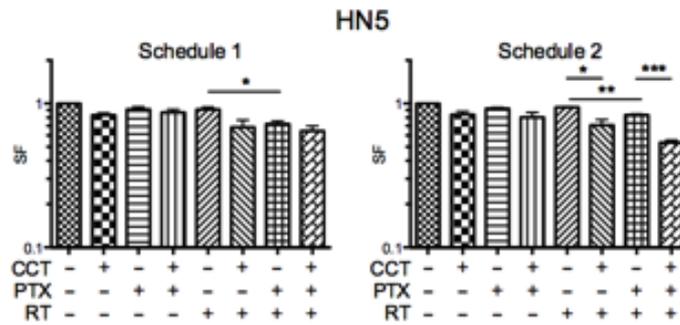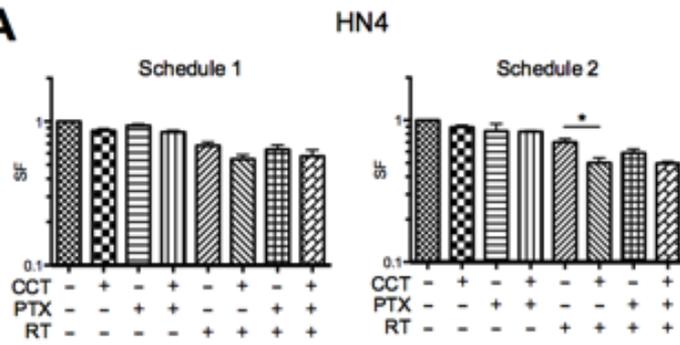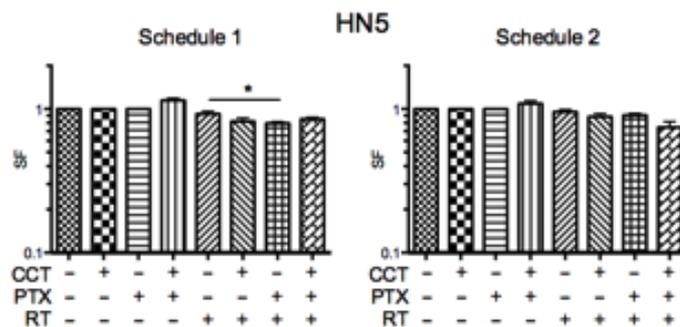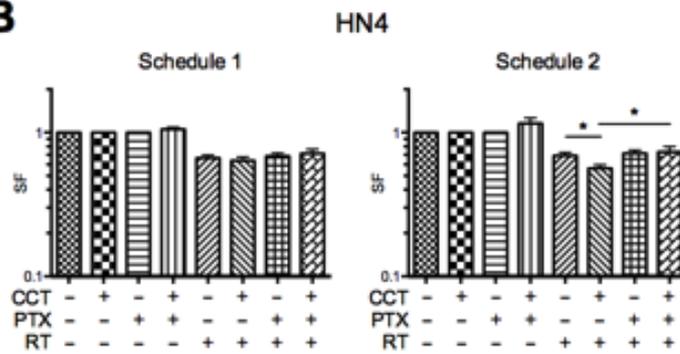
Supplementary Figure S3
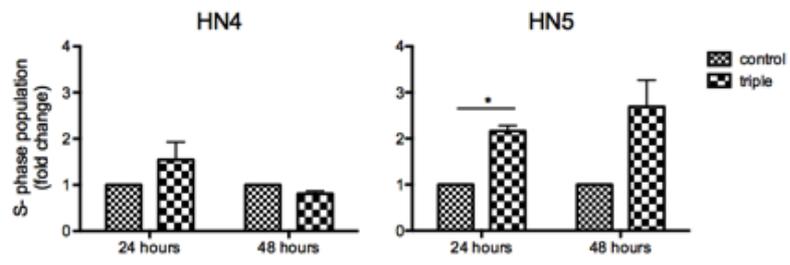
Supplementary Figure S4

Supplementary Figure S5

nuclear CHK1

cytoplasmic CHK1

nuclear p-CHK1

cytoplasmic p-CHK1

p-ATM

Ki67

Survivin

Low expression   High expression